CHALMERS
UNIVERSITY OF TECHNOLOGY

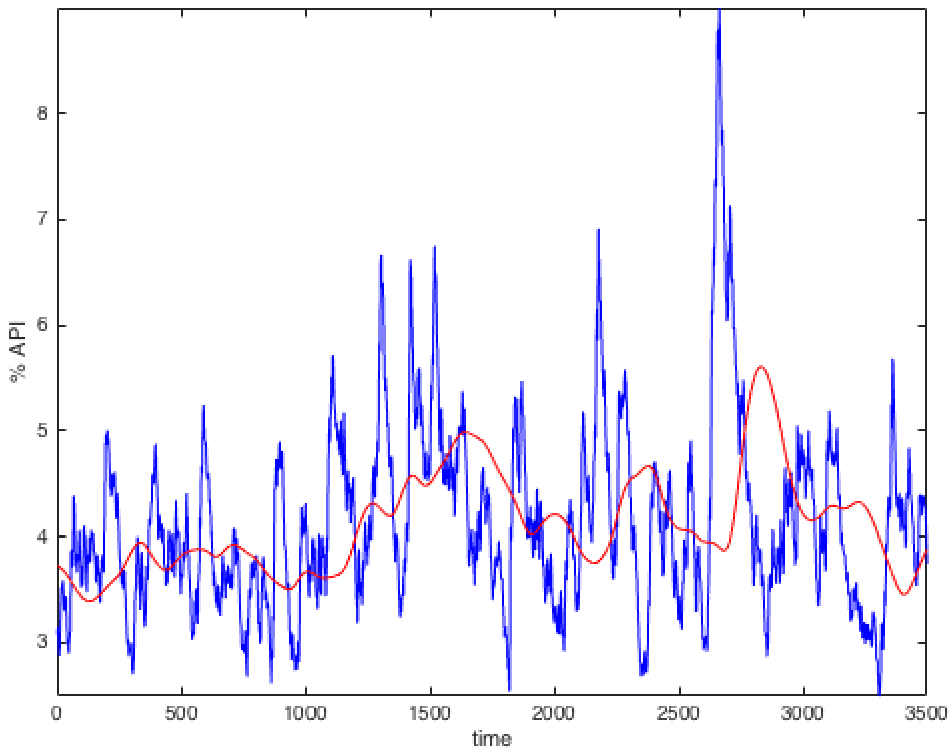

Modelling of Continuous Powder Mixing

ULRIK KÄLLBLAD

Department of Chemical Engineering
CHALMERS UNIVERSITY OF TECHNOLOGY
Gothenburg, Sweden 2016

Master's thesis 2016

Modelling of Continuous Powder Mixing

ULRIK KÄLLBLAD

Department of Chemical Engineering
Department of Mathematical Sciences
Chalmers University of Technology
Gothenburg, Sweden 2016

Modelling of Continuous Powder Mixing
ULRIK KÄLLBLAD

© ULRIK KÄLLBLAD, 2016.

Supervisor: Johan Remmelgas, AstraZeneca
Examiner: Anders Rasmuson, Department of Chemical Engineering

Master's Thesis 2016
Department of Chemical Engineering
Department of Mathematical Sciences
Chalmers University of Technology
SE-412 96 Gothenburg
Telephone +46 31 772 1000

Cover: Concentration of API in the mass flow going into a continuous mixer (blue curve) and the simulated concentration of API in the mass flow going out from the mixer (red curve). Time is in seconds.

Gothenburg, Sweden 2016

Acknowledgement

I want to thank my supervisor at AstraZeneca, Johan Remmelgas, for his enthusiastic involvement, guidance and assistance. I also want to thank my examiner at Chalmers University of Technology, Anders Rasmuson, for his helpful advice and guidance.

Abstract

The pharmaceutical industry has in recent years showed a lot of interest in replacing current batch manufacturing methods with continuous ones. This requires more knowledge about powder mixing and how to model powder behaviour. In this thesis a model for continuous powder mixing is developed. The aim is to find a model that can predict how fluctuations in the feeder flow rate affects the powder mixture at the outlet of a continuous mixer. To achieve this, two models are used. One model describes the mixer as continuously stirred tank reactors in series and one using the axial dispersion model to describe the powder flow. The system that is modelled is a CDC-50 continuous mixer at GEA in Belgium. Runs were performed with different impeller rates and number of impeller blades. The results show that both models can be used to model continuous powder mixing in this specific continuous mixer. The results also show that higher impeller rates and fewer impeller blades resulted in shorter residence times and less mixing. The effect of feeder stops is also investigated and the results show that short stops can occur without having to discard tablets.

Contents

1 Introduction

In pharmaceutical tablet manufacturing it is important to produce tablets with small variability. A small deviation in concentration of some ingredient can affect the therapeutic effect. To assure the patients' safety it is vital for the pharmaceutical companies to be able to control and understand the manufacturing process of tablets.

Most tablets in the pharmaceutical industry are currently produced using batch process manufacturing. This process typically includes a number of steps. The first step is to mix all particles together until a homogeneous mixture is obtained. The next step is to form granules by collecting powder particles together. This step is called granulation and is done to prevent the mixture from segregating and improve fluidity. The powder is then compressed into tablets and the final step is to give them a protective coating. A downside of this type of method is that it involves many discrete steps in which the powder needs to be stored or moved between different containers, which can cause the mixture to segregate. An alternative for batch processing, that has gained more and more attention in recent years is continuous tablet manufacturing. In a continuous manufacturing process, one or more steps in the batch process are performed continuously, without stops between the steps.

The disadvantages of continuous manufacturing are mainly expensive equipment and underdeveloped methods to control the process. However, manufacturing of tablets has some major advantages compared to batch manufacturing including better mixing of segregating materials and decrease in production costs. In addition the continuous manufacturing line usually require less space and the manufacturing process involves fewer steps which leads to shorter production time. Despite the predominant advantages, continuous manufacturing is not used extensively in the pharmaceutical industry. However guidance and support from authorities has made it easier for companies to implement continuous manufacturing in their production line the interest in this alternative production method has increased. This has led to a need for better understanding of powder mixing in a continuous manufacturing process.

Mixing of powder is a process with many different forces involved. Forces include collisions, friction and interparticular forces such as van der Waals forces and electrostatic forces. Since the particles are very small, around 50 μm, air flows does also have an important influence on the particles. The amount of moisture in the powder and how packed the particles are also affect the powder properties. With all these parameters it is very difficult to model powder mixing and a fundamental understanding of powder behaviour is still lacking.

The optimal way to model powder mixing would be to account for every force that acts on each individual particle and then simulate how the particles will behave. Many models are built on this idea, often simplified to include fewer forces. One such method is called the discrete element method in which stresses and displacements for a large number of particles are calculated. A discrete element method was developed in [Flo15] to better understand mixing in a fluidized powder flow. The downside of particulate models are mainly the high computational cost needed to simulate larger amount of particles. The maximum number of particles that currently can be simulated for a reasonable cost is around 100 millions [Jaj13]. If the size of the particles are approximated as spheres with 50 μm in diameter and the volume of the mixer is 1 m^3, the number of particles in the mixer is $6 \cdot 10^{13}$, which is much more than what currently can be simulated.

Stochastic models has also been proposed to describe powder mixture in a blender. A stochastic model tries to give probabilities of different events to happen in a process. In a powder mixing process these events could be particles moving between different compartments of the mixer. Berthiaux developed [Ber04] such a model to describe particle movements in a mixer. The mixer was divided into different compartments and probabilities for powder to travel between the compartments were calculated. This kind of model is suitable for mixers that have clear geometrical compartments, but otherwise it might be difficult to define the transition probabilities. One way to to calculate the transition probabilities is to use computational fluid dynamic type models. These methods struggles if the powder does not behave as a fluid and the lack of fundamental understanding of powder behaviour makes it also difficult to consider powder properties such as deformation of particles.

In this thesis a continuous manufacturing process is analysed in which materials are charged into a blender and mixing takes place as the material travels through the blender. The blender is connected to a tablet compression machine that compresses the powder into tablets. In this thesis the focus will be on developing a model that can predict how variations in feeder flow rate affects the powder mixture at the outflow of the mixer. The models described above are good at modelling powder mixing on a detailed level. For our purpose however, a simpler modelling approach can be used. The approach that will be used is built on the residence time distribution of the mixer, which is the probability distribution of how long time a particle will spend in the mixer. This is a common approach in chemical engineering literature [Gao11], [Eng16] and has been used before to model different continuous mixers.

2 Model setup

In this section we introduce the theoretical model that will be used to study the continuous mixing process. The objective of the model is to be able to predict the concentration of API at the outflow of the mixer given the inlet concentration. Four different model approaches will be used. The first one models the mixer as continuously stirred tank reactors in series. The second model approach is to use a plug flow reactor model to describe the mixer. The last modelling approach is to use the axial dispersion model with open and closed boundary conditions to model the powder flow. All these models were originally developed to describe how different fluids spread in a tube, but since a powder flow has many similarities with a fluid the use of the models can be motivated.

2.1 Residence time distribution

In a continuous powder mixing process, the particles that enter the system at a given time, will not leave the system at the same time. Some particles will go through faster and others will stay longer. A distribution of the time a particle spends in a system can be described by the residence time distribution (RTD). The residence time distribution, denoted by $E(t)$, is a probability distribution of how long time a particle will spend in the system. With this definition the probability that a particle leaves the system in the time interval t to $t + dt$, is $P(t,t + dt)$ given by

$$P(t,t + dt) = \int_{t}^{t+dt} E(t)dt. \tag{1}$$

The residence time distribution can be obtained experimentally by a pulse test. In a pulse test a measurable substance, for example a colour, is added at the inlet of the system. To approximate a pulse the substance is added as quickly as possible so that all particles are added at the same time. The concentration of the added substance is then recorded at the end of the system and the residence time distribution is obtained by

$$E(t) = \frac{C_{out}(t)}{\int_0^\infty C_{out}(t)dt}, \tag{2}$$

where $E(t)$ is the residence time distribution and C_{out} is the measured concentration going out from the system. It is very important that the pulse added does not affect the behaviour of the powder flow. The amount of powder added should hence be small but still detectable.

An important value related to a probability distribution is the expected value or the mean value defined as

$$\bar{t} = \int_0^\infty tE(t)dt. \tag{3}$$

For a powder flow this is the average time that the particles will spend in the mixer and hence a measure of how quickly the flow travels through the mixer.

2.1.1 Convolution theorem

In a system where the residence time distribution and the concentration of a substance going into the system is known, the concentration of the substance in the flow going out from the system is given by the convolution theorem

$$C_{out}(t) = \int_0^t C_{in}(s)E(t-s)ds, \tag{4}$$

where $C_{out}(t)$ is the concentration going out from the system, $C_{in}(t)$ is the concentration going in to the system and $E(t)$ is the RTD function of the system.

2.2 Residence time distribution models

Equation (4) will be used to predict the concentration of API at the outflow of the mixer. In order to use this formula, a closed form function describing the residence time distribution needs to be defined or alternatively defining a numerical residence time distribution function. To find a suitable function, four different models will be used to describe the residence time distribution of the mixer, namely continuously stirred tank reactors in series model, plug flow reactor model and the axial dispersion model with open and closed boundary conditions. A compact closed form solution can be derived for the three first models. A closed form solution for the axial dispersion model with closed boundary conditions also can be derived, but the derivation is extensive and the expression obtained is very long. Hence the axial dispersion model with closed boundary conditions is preferable solved numerically.

2.2.1 Continuously stirred tank reactors in series

A continuously stirred tank reactor (CSTR) is a mixing tank which is perfectly mixed, meaning that the concentration of a substance is the same everywhere in the tank. If many CSTR are connected in series they can be used to model the RTD curve of a mixing system. The RTD curve for N CSTRs in series is given by

$$E(t) = \frac{t^{N-1}e^{-\frac{t}{\tau}}}{(N-1)!\tau^N}, \tag{5}$$

where τ is a parameter. See figure 1 for examples of RTD curves for different number of CSTRs in series. A higher number of CSTRs in series means a sharper curve and less mixing. A smaller number of CSTRs in series means a more spread out curve and more mixing. The mean residence time distribution for the N CSTR in series model is equal to

$$\bar{t} = N\tau. \tag{6}$$

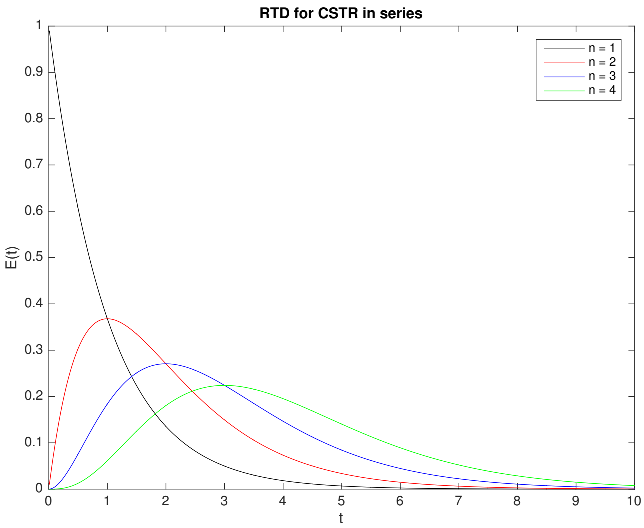

Figure 1: RTD curves for different number of CSTR in series. The x-axis represents time in seconds.

2.2.2 Plug flow reactor

A plug flow reactor (PFR) model is a theoretical model that attempts to describe how liquids travel through a pipe. It assumes that no mixing takes place in the axial direction and that perfect mixing takes place in the radial direction. The concentration of a substance as a function of space and time in a plug flow reactor can mathematically be expressed as

$$c(x,t+dt) = c(x-vdt,t), \tag{7}$$

where v is the bulk speed of the flow in the pipe. Physically this equation means that the model only transports the flow with speed v and does not change it. Therefore the PFR model can be used to model parts of the mixing process where the powder primarily is transported and only a small amount of mixing in axial direction takes place.

2.2.3 Axial dispersion model

The axial dispersion model describes how the concentration of a substance spreads through a pipe. It assumes that the substance only moves due to the bulk velocity of the particle flow, referred to the advection part and the difference in concentration referred to the dispersion part. In this approach the dispersion part is modelled to behave as diffusion in a fluid.

The axial dispersion model can be derived using a control volume. The control volume is defined as an infinitesimal thin slice of the mixer, of length L, in which the flow takes place. The change in concentration in this small control volume is equal to the difference between the concentration going into, and the concentration going out from the control volume. This can be formulated in terms of flux as

$$\frac{\partial c}{\partial t} + \frac{\partial}{\partial x}(j) = 0, \tag{8}$$

where c is the concentration in the control volume, j is the flux through the control volume, t is time and x is the axial position in the mixer. In the axial dispersion model the flux is dependent on advection and dispersion so the flux can be written as

$$j = j_{advection} + j_{dispersion}. \tag{9}$$

The advection flux is defined as

$$j_{advection} = vc, \tag{10}$$

where v is the average velocity of all particles in the control volume, often called the bulk velocity. The dispersion flux is taken from Ficks' first law of diffusion and is given by

$$j_{diffusion} = -D\frac{\partial c}{\partial x}, \tag{11}$$

where D is the dispersion coefficient that determines how much the tracer will spread due to dispersion. Substituting equation (10) and equation (11) into equation (8) gives

$$\frac{\partial c}{\partial t} + \frac{\partial}{\partial x}(vc - D\frac{\partial c}{\partial x}) = 0. \tag{12}$$

which for a constant dispersion coefficient and bulk velocity can be written as

$$\frac{\partial c}{\partial t} + v\frac{\partial c}{\partial x} = D\frac{\partial^2 c}{\partial x^2}. \tag{13}$$

The axial dispersion is closely related to the CSTR model and the PFR model. Setting $D = 0$ means no mixing at all and a PFR model and setting $D = \infty$ means perfect mixing and a CSTR model.

Equation 12 can be made dimensionless by the following variable substitution

$$\theta = t\frac{v}{L} \tag{14}$$

and

$$\xi = \frac{x}{L}. \tag{15}$$

to obtain

$$\frac{\partial c}{\partial \theta} + \frac{\partial c}{\partial \xi} = \frac{1}{Pe}\frac{\partial^2 c}{\partial \theta^2} \tag{16}$$

where $Pe = \frac{Lv}{D}$ is the so called Peclet number. The Peclet number is a ratio of how much of the transport that is due to advection and how much that is due to dispersion. A small Peclet number indicates large amount of mixing and a large Peclet number indicates less mixing.

2.2.4 Boundary conditions

The solution to the axial dispersion model depends on the boundary conditions that are used. Three boundary conditions that are commonly used when modelling powder flows are Dirichlet, open and closed boundary conditions. The Dirichlet boundary condition sets the concentration at the boundary to a specific value, the open boundary condition means that there is dispersion both upstream and downstream of the mixer and the closed boundary condition means that there is no dispersion upstream or downstream of the mixer. The closed and open boundary conditions are illustrated in figure 2.

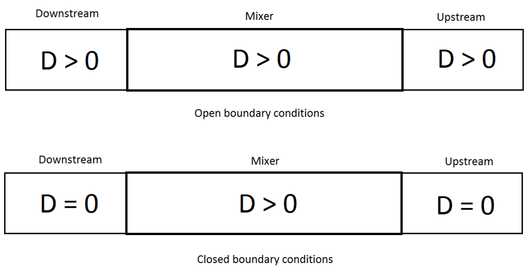

Figure 2: Illustration of open and closed boundary conditions. With open boundary conditions diffusion takes place upstream and downstream of the mixer and with closed boundary conditions diffusion only takes place inside of the mixer.

The open boundary condition can mathematically be formulated as

$$c(t{,}x) = 0 \text{ for } x \to \pm\infty \tag{17}$$

and the closed boundary condition can be formulated as

$$\frac{\partial c}{\partial t} = 0 \text{ for } x = 0{,}L. \tag{18}$$

2.2.5 Closed form solution to the axial dispersion model

For the case of open boundary conditions, equation 6 has an closed form solution. Since we are interested in the concentration at the end of the mixer, x is set to L, and the solution is given by

$$E(t{,}x) = \frac{L}{\sqrt{4\pi t D}} e^{-\frac{(L-vt)^2}{4tD}}. \tag{19}$$

See APPENDIX A for derivation of equation (19).

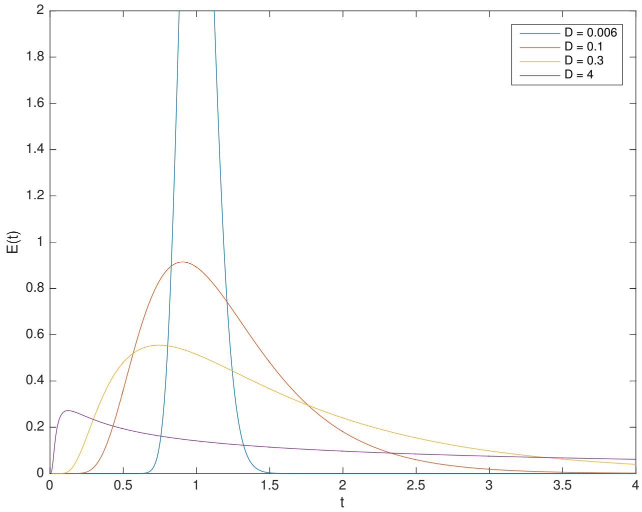

Figure 3: RTD curves for the axial dispersion model with open boundary conditions for different dispersion coefficient. Lower values of the dispersion coefficient results in a more plug flow like behaviour and higher values results in a more continuously stirred tank reactor behaviour.

2.3 Axial dispersion model with closed boundary conditions

The axial dispersion model with closed boundary conditions has no closed form solution. In this case the equation is therefore solved numerically by the finite difference method. The finite difference method is a numerical method used to solve differential equations. First the mixer is discretized by forming a grid. The x axis of the grid is the spatial positions in the mixer and the y axis of the grid is the time steps.

At each grid point the derivatives are approximated by their Taylor expansion. The approximations can either be explicit or implicit. An explicit approximation means that the current time step is used in the approximations of the spatial derivatives and an implicit approximation means that the next time step is used in the approximations of the spatial derivatives. In this thesis an implicit finite difference method has been used. The advantage of an implicit method is that it is stable regardless parameter choice, spatial step length or time step length. The finite difference method is said to be stable if it damps out, instead of magnifying, small fluctuations in the input data. The disadvantage of an implicit method is that there is no explicit expression for the concentration in the next time step and a system of equations needs to be solved each iteration step.

A problem that might occur for flows with Peclet number greater than 2 is that the approximation of the advection term fails to converge. As can be seen in the result section, the Peclet number for every run is greater than 2. To overcome this problem a backward difference is used to approximate the advection term. The large drawback of the backward difference is that it is inaccurate.

The following implicit approximations for the derivatives in equation 11 has been made.

$$\frac{\partial c}{\partial t} \approx \frac{c_m^{n+1} - c_m^n}{\Delta t}, \tag{20}$$

$$\frac{\partial c}{\partial x} \approx \frac{c_m^{n+1} - c_{m-1}^{n+1}}{\Delta x}, \tag{21}$$

$$\frac{\partial^2 c}{\partial x^2} \approx \frac{c_{m+1}^{n+1} - 2c_m^{n+1} + c_{m-1}^{n+1}}{(\Delta x)^2}. \tag{22}$$

In the approximations above n is the time position, m is the spatial position, Δt is the space between each time position, Δx is the space between each spatial position and c_m^n is the concentration at spatial position m and time position n.

By substituting the approximations (20),(21) and (22) into equation (13), the following equation is obtained

$$\frac{c_m^{n+1} - c_m^n}{\Delta t} + v\frac{c_m^{n+1} - c_{m-1}^{n+1}}{\Delta x} = D\frac{c_{m-1}^{n+1} - 2c_m^{n+1} + c_{m+1}^{n+1}}{(\Delta x)^2} \tag{23}$$

By moving all the terms with time position $n + 1$ to the left side and all the terms with time position n to the right side this can be written as

$$c_{m-1}^{n+1}(-k_1 - k_2) + c_m^{n+1}(1 + 2k_2 + k_1) + c_{m+1}^{n+1}(-k_2) = c_m^n, \tag{24}$$

with

$$k_1 = v\frac{\Delta t}{\Delta x} \tag{25}$$

and

$$k_2 = D\frac{\Delta t}{(\Delta x)^2}. \tag{26}$$

This equation can be written in matrix form as

$$A\boldsymbol{c}^{n+1} = \boldsymbol{c}^n, \tag{27}$$

where

$$\boldsymbol{c}^n = \begin{bmatrix} c_1^n & c_2^n & c_3^n & \ldots & c_{m-1}^n & c_m^n \end{bmatrix}^T,$$

$$\boldsymbol{c}^{n+1} = \begin{bmatrix} c_1^{n+1} & c_2^{n+1} & c_3^{n+1} & \ldots & c_{m-1}^{n+1} & c_m^{n+1} \end{bmatrix}^T,$$

$$\mathrm{A} = \begin{bmatrix} c_{in} & 0 & 0 & \ldots & 0 & 0 & 0 & 0 \\ -k1 - k2, & 1 + k_1 + k_2, & -k_2 & 0 & \ldots & 0 & 0 & 0 \\ 0 & -k1 - k2, & 1 + k_1 + k_2, & -k_2 & 0 & \ldots & 0 & 0 \\ 0 & 0 & -k1 - k2, & 1 + k_1 + k_2, & -k_2 & 0 & \ldots & 0 \\ \vdots & & & & & & & \vdots \\ 0 & \ldots & 0 & 0 & 0 & -k1 - k2, & 1 + k_1 + k_2, & -k_2 \\ 0 & 0 & \ldots & 0 & 0 & 0 & 0 & 1 \end{bmatrix}$$

Using Dirichlet boundary conditions at the first boundary and closed boundary conditions at the second boundary results in the first row and the last row, respectively, in the matrix. The matrix is a tridiagonal matrix with dimensions mxm. Using Matlab this matrix equation is solved for each time step.

3 Experimental equipment and methods

In this section the continuous mixer used in the experiments is described, the different mixer settings for each run are stated and the method used to extract RTD curves for the mixer is explained.

The RTD measurements were performed on a CDC-50 continuous production line at GEA Wommelgem in Belgium. The production line consisted of two cylindrical mixers connected to each other. In each mixer a rotating impeller mixed and transported the powder. Paddles were attached to each impeller and the number of paddles could be varied and set at different angles. Five feeders were used to feed the first mixer with materials. One of these feeders added API to the mixer. A sixth feeder was also placed between mixer one and mixer two, adding a lubricant to prevent the powder from sticking to the tablet machine. A schematic figure of the continuous production line is presented in figure 4. Impeller rates and the number of blades attached to the impellers for each run are summarized in table 1.

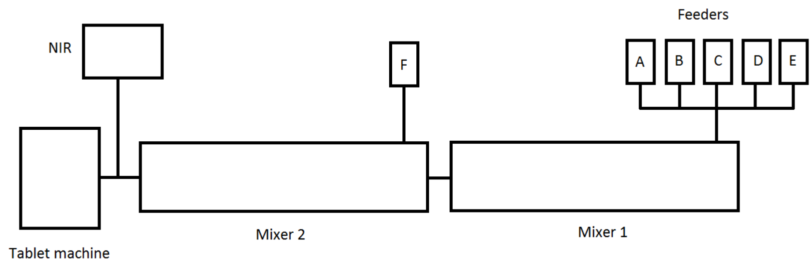

Figure 4: Schematic figure of the continuous production line used in the measurements.

In each run a small but readily detectable amount of API was added to the inlet of the mixer at one point in time. In order to approximate a pulse test, the material was added as quickly as possible. This was done both at the inlet of the first mixer and at the inlet of the second mixer. The response was measured at the outlet of the second mixer by a near infrared spectrometer.

Run	speed M1 [rpm]	speed M2 [rpm]	blades M1	blades M2
A	300	250	16	16
B	200	250	16	16
C	400	250	16	16
D	400	250	8	8
E	200	250	8	8
F	300	250	8	8
G	300	200	8	8
H	300	300	8	8
I	300	250	20	20
J	200	250	20	20
K	400	250	20	20

Table 1: Impeller speed, measured in revolutions per minute, and number of blades attached to the impeller in each mixer for each run. M1 denotes mixer 1, M2 denotes mixer two.

3.1 Analysis of near infrared ligth spectra

To measure the response of the pulse test at the outlet of the mixer, near infrared (NIR) spectroscopy was used. Near infrared light (780-2500 nanometre) can excite vibrations in chemical bonds. Different chemical bonds requires different amounts of energy to start to vibrate, and therefore different bonds absorb different wavelengths of light. Some substances are known to contain specific bonds and the absorption spectrum can hence be used to get information about what substances there are in a sample.

A near infrared absorption spectrum is not straight forward to analyse since it contains vibrational overtones and other noise. An analysing method is hence required to get out useful information from a near infrared absorption spectrum. Below the analysing method used in this thesis is explained. The goal of the method is to be able to give a measure of how much API there is in the powder at the outflow of the mixer. Usually when analysing near infrared spectra, principal component analysis is used, but since the focus in this thesis is on modelling and not NIR data analysis, the simpler method described below is used.

3.1.1 Average absorbance method

To see which wavelengths that API absorbs most, a NIR measurement of a sample containing only API is performed. The absorbtion spectrum has a peak, around 50 nanometres wide, which indicates that the API absorbs these wavelengths more than other wavelengths.

When the continuous mixer was running, the NIR spectrometer made a measurement every second with 4 nanometer wavelength accuracy. To remove differences between measurements, that is not due to variation in composition of the sample, each absorption value are subtracted by the mean of all absorption values for that measurement and divided by the standard deviation for all absorption values for that measurement. This transformation is called a standard normal variate transformation.

To get a measure of how much API that the powder at the outflow contained the average absorption over a wavelength interval of 50 nanometres was calculated for each measurement. In figure 5 this average is presented for run A. The higher value starting around time point 500 is the pulse response for the first pulse test in run A. The experimentally obtained residence time distribution is then obtained by normalizing this pulse response by dividing each value with the area under the graph. The pulse response for the second mixer can be seen as the top starting around time point 1000. The smaller response is due to that less API was added in the second pulse test each run. The same procedure was done for all runs and the extracted RTD curves can be found in the result and discussion chapter.

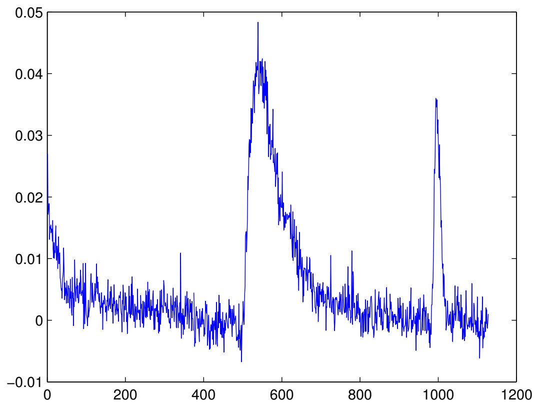

Figure 5: The average intensity from run A over wavelengths of the peak of 50 nanometres for all measurements. The x-axis represents time and the y-axis represents the average absorbtion.

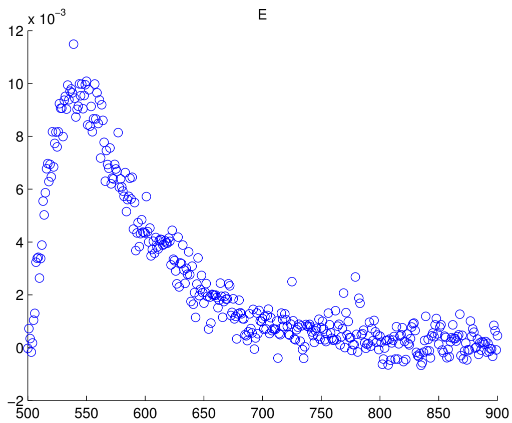

Figure 6: The average intensity from run A over wavelengths of the peak of 50 nanometres for measurements between 500-900. The x-axis represents time and the y-axis represents the average absorbtion.

4 Results and discussion

The results include the RTD curves extracted from the NIR data and curve fitting of the RTD curves using both 2 CSTR in series model and the axial dispersion model with open boundary conditions. The effect of how different mixer settings affect the API concentration in the outflow is investigated. In particular the 2 CSTR in series model is used to simulate how feeder stops affect the concentration of API in the outflow of the mixer. The 2 CSTR in series model is also used to investigate the damping ability of the mixer. The axial dispersion model with closed boundary conditions, solved by the finite difference method, is used to simulate how interruptions in feeder operation affects the API concentration in the outflow. The models are also used to simulate a full run using real feeder flow rate data.

4.1 RTD curves

In each run two pulse tests were performed as described in chapter 3. The RTD curves extracted from these pulse tests for run A-F,I and K are presented in figure 8. The RTD curves were extracted using the method described in chapter 3. Impeller speeds and the number of blades attached during these runs are presented in table 1. Since the focus is on modelling the concentration of API which travels through both mixers, only RTD curves for both mixers combined are presented and analysed. The pulse response for the second pulse was not as informative as the first pulse. This was due to that more API was added in the first pulse and the response was therefore easier to detect by the NIR spectrometer.

4.2 Curve fitting

Two different approaches are used when fitting the RTD data. The first approach includes the measurements from that the pulse is added until the first particles reach the end the mixer. The time it takes for the first particles of the pulse to reach the end of the mixer, is called dead time.

The second approach do not consider the dead time and makes a curve fit of the measurements from the time that the first particles are detected at the end of the mixer. To account for the dead time in the model a PFR that only transports the powder is used. With this approach the parameters v and L looses their physical meaning but better curve fits are obtained.

4.2.1 With dead time

Since the point in time when the pulses were added is not known, three different dead times are simulated for run A; 60 seconds, 120 seconds and 180 seconds. The parameters from the curve fitting is presented in table 2. As can be seen in figure 7, the ability of the model to fit the curve becomes worse as the dead time increases.

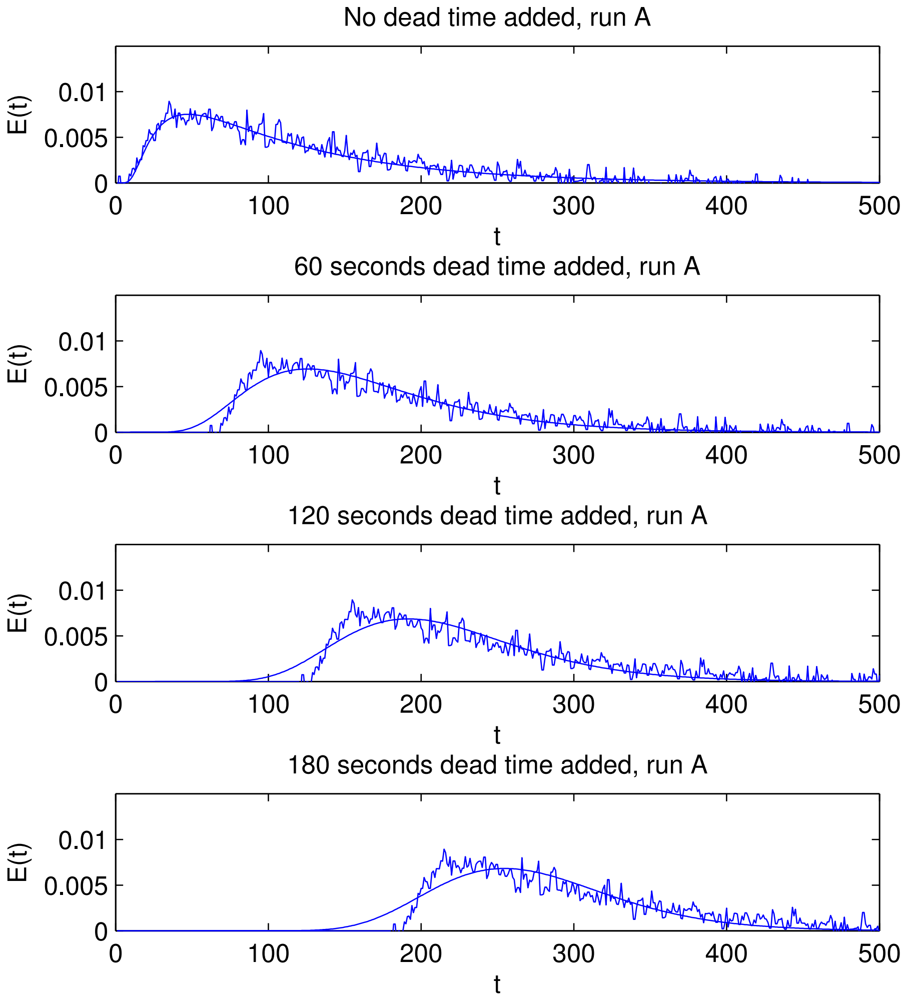

Figure 7: Curve fitting of the RTD from run A, adding different dead times.

Dead time	v	D	L
0	0.0056	7.84e-04	0.37
60	0.0071	6.32e-04	0.97
120	0.0117	0.0012	2.34
180	0.0067	2.97e-04	1.74

Table 2: The estimation parameters for the axial dispersion model with open boundary conditions using the RTD curve from run A with different dead times. The x-axis represents time in seconds.

4.2.2 Without dead time

The 2 CSTR in series model and the axial dispersion model with open boundary conditions were used to model the RTD curves extracted from the NIR data. The RTD function for 2 CSTR in series is given by

$$E(t) = \frac{t}{\tau^2} e^{-t/\tau} \tag{28}$$

where τ is the estimated parameter. For the axial dispersion model with open boundary conditions the estimated parameters are v,D and L. The values of the parameters were determined by a least square method. It was also tested if a model with more CSTR in series would give a better description of the data. For the experiments in this thesis, the axial dispersion model described the data better in every case. In some cases it was better to use a model with more CSTR in series compared to a model with only 2 CSTR in series. But in some cases a model with 2 CSTR in series described the data better and since it is easier to work with a model with only 2 CSTR in series this model has been used. In table 3 the estimated τ for the 2 CSTR in series model and v,D, L and the Peclet number for the axial dispersion model are presented.

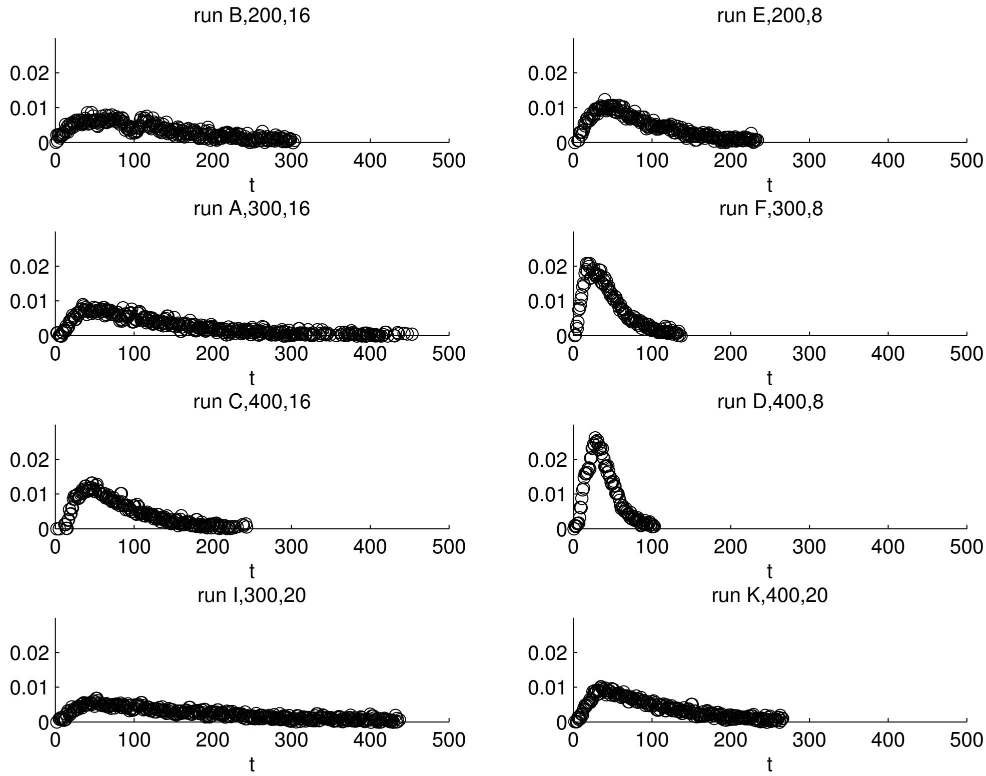

Figure 8: Experimentally obtained RTD curves for each run. Note that the time it takes for the first particles from the pulse to reach the end of the mixer is not included. The x-axis represents time in seconds.

Run	$\tau[s]$	v [m/s]	D [m^2/s]	L [m]	Peclet number
A	54.33	0.0056	7.84e-04	0.37	2.66
B	56.79	0.0023	1.62e-04	0.15	2.15
C	40.59	0.0137	0.0023	0.75	4.49
D	21.27	0.0987	0.0460	3.06	6.57
E	40.86	0.0072	8.77e-04	0.38	3.12
F	21.70	0.0185	0.0028	0.54	3.53
I	73.82	0.0109	0.0052	0.93	1.96
K	45.40	0.0053	5.97e-04	0.30	2.68

Table 3: Estimation of parameters for 2 CSTR in series and axial dispersion models with open boundary conditions. The parameters are estimated using the data in figure 8

In figure 9 and 10, a visual comparison between model predictions and the experimental data of run C is made. Similar results were obtained for each run and it was concluded that the axial dispersion model was better at modelling the data. In figure 11, RTD curves for each run modelled by the axial dispersion model with open boundary conditions are presented.

Even though the axial dispersion model with closed boundary conditions is better at describing the RTD curves, the 2 CSTR in series model performs almost equally well. Since the 2 CSTR in series model is easier to work with, it is the most used model in the simulations and derivations of analytical expressions.

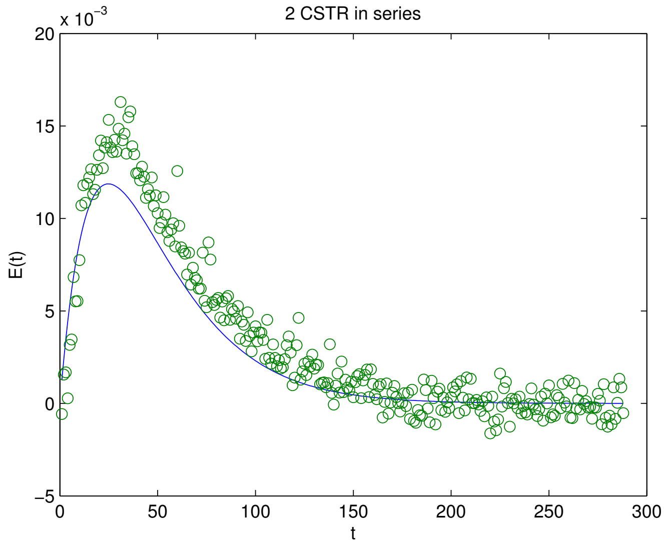

Figure 9: Curve fitting of extracted RTD curve for run A using the 2 CSTR in series model. The x-axis represents time in seconds.

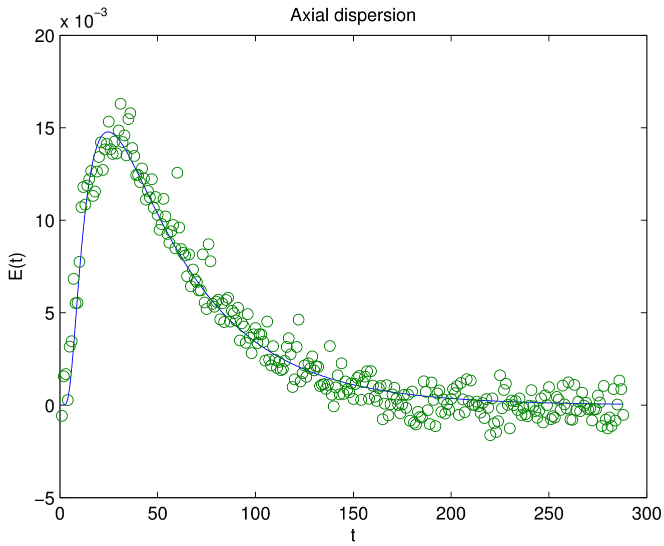

Figure 10: Curve fitting of extracted RTD curve for run A using the closed form solution to the axial dispersion model with open boundary conditions. The x-axis represents time in seconds.

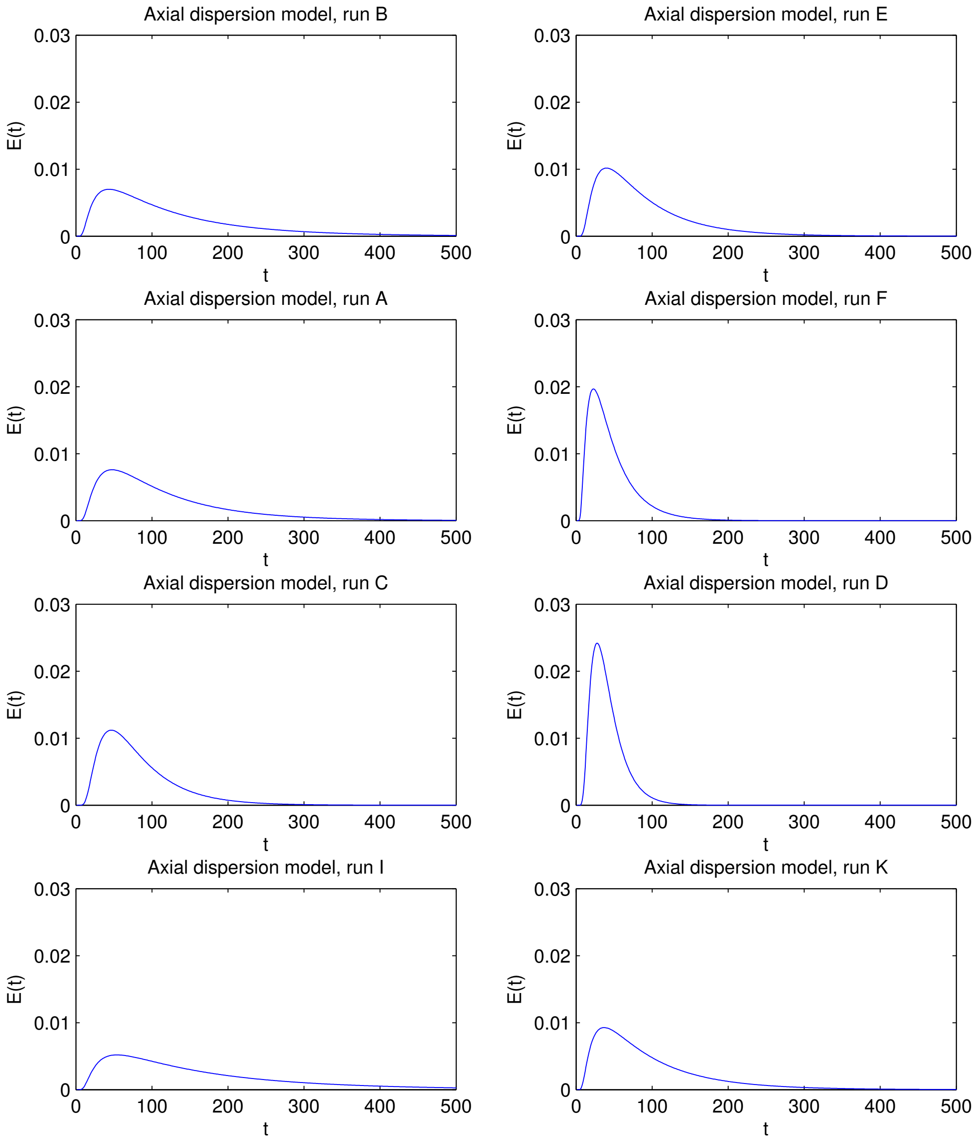

Figure 11: RTD curves for each run modelled by axial dispersion model with open boundary conditions. Note that the time it takes for the first particles from the pulse to reach the end of the mixer is not included. The x-axis represents time in seconds.

4.2.3 Prediction of τ in the 2 CSTR in series model

Interestingly the parameters estimated from the experimental data seem to follow a pattern. If this pattern is known the RTD curve for a new mixer setting can be predicted without the need to perform a pulse test. A linear interpolation was made on the values of τ presented in table 3. The results of this interpolation is presented in figure 12. A higher impeller rate results in a lower τ and a higher number of blades results in a higher τ. The number of blades attached to the mixer has larger effect on τ for lower impeller rates and the impeller rate has more effect on τ for higher number of blades.

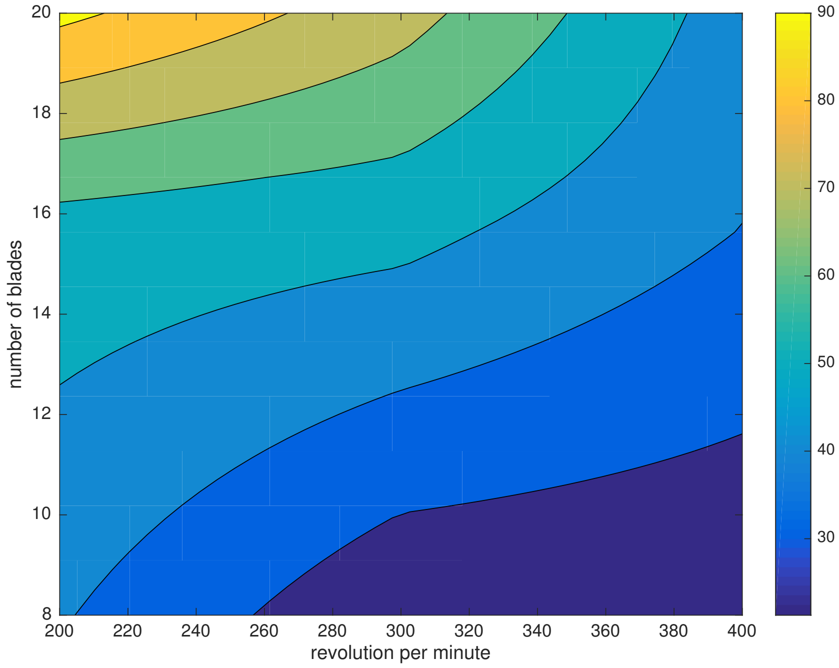

Figure 12: Linear interpolation of τ in the 2 CSTR in series model. The measured values were obtained from table 3.

4.3 Simulations

Simulations have been performed to evaluate how different feeder settings and different parameter values affect the mixing. Simulations were performed using the convolution theorem with the 2 CSTR in series model and the axial dispersion model with open boundary conditions. Simulations for the axial dispersion model with closed boundary conditions solved by the finite difference method were also performed.

4.3.1 The 2 CSTR in series model

In figure 13 two simulations using the 2 CSTR in series model with real values of the API concentration in the inflow, data are presented. The simulation was performed to show how a higher versus a lower value of τ affects the performance of the mixer. The largest and smallest value of the estimated parameters in table 1 were selected. The result shows that a higher value of the parameter τ results in a longer mean residence time and more damping of the fluctuations.

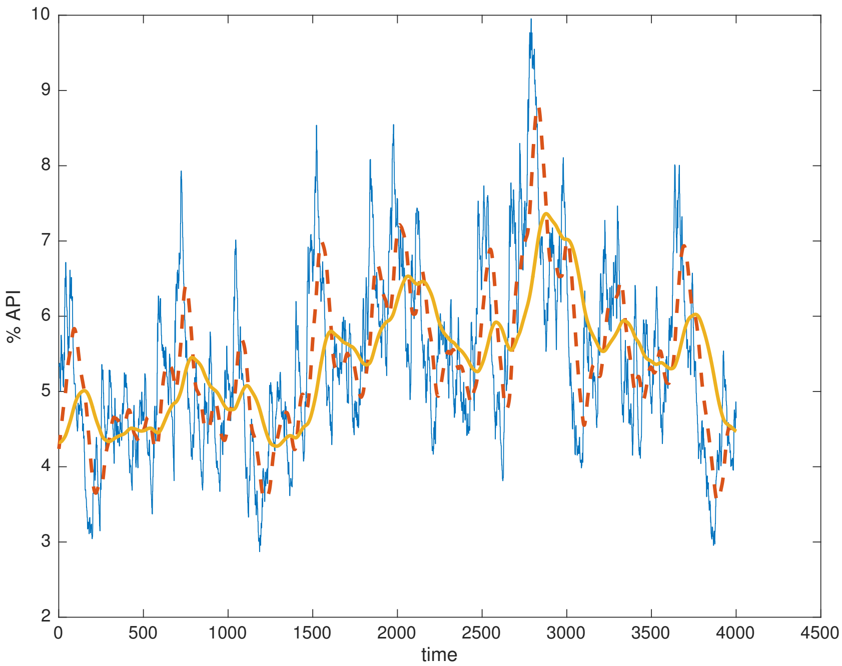

Figure 13: Simulation of run A using the 2 CSTR in series model with parameters τ = 73.82 (yellow curve) and τ = 21.27 (red striped curve). The blue line represents the API concentration in the inflow to the mixer. Note that the time it takes for the first particles from the pulse to reach the end of the mixer is not included. The x-axis represents time in seconds.

The 2 CSTR in series model was used to simulate how a feeder interruption affected the API concentration in the outflow of the mixer. A feeder interruption is simply when the API feeder does not transport any material into the mixer over a period of time. In figure 14 four different durations for the feeder interruptions are simulated. One can see that the mixer can handle short feeder interruptions but longer feeder interruptions results in large deviations of the API concentration in the outflow. In the simulation the parameter were set to $\tau = 54.33$.

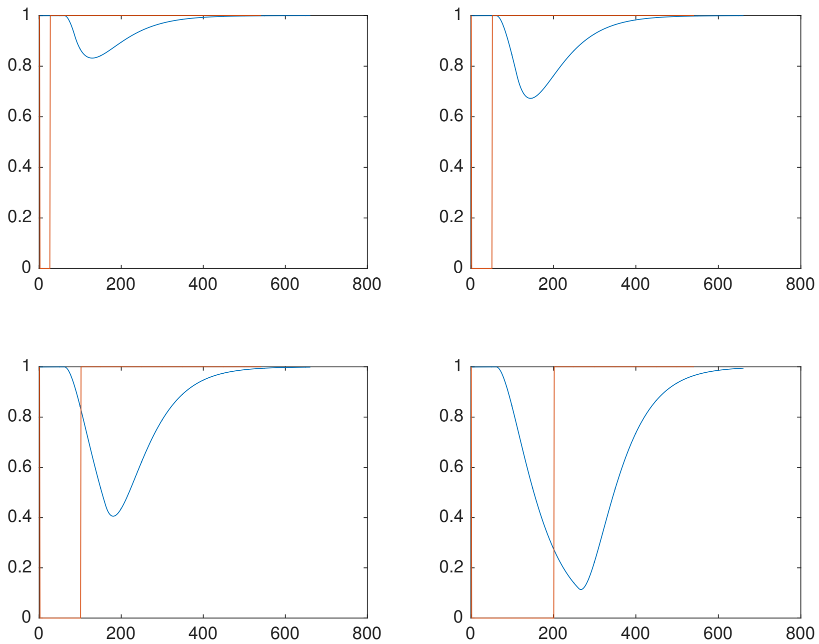

Figure 14: Feeder interruptions of different length simulated by the 2 CSTR in series model with $\tau = 54.33$. The length of the feeder interruptions are 25, 50, 100 and 200 seconds. An arbitrary time it takes for the first particles from the pulse to reach the end of the mixer is set to 60 seconds.

The maximum duration of the feeder interruption in order for the nominal concentration of the API not to go below 98% was also calculated using the 2 CSTR in series model. If the concentration of API before the interruption was constant, the nominal concentration of API in the outflow after the feeder interruption is

$$c_{API}(t) = 100(1 - \int_0^t \frac{s}{\tau^2} e^{-s/\tau} ds) \tag{29}$$

where t is the time after the feeder stops feeding API into the mixer. In figure 15 equation (29) is plotted. The result shows that for this mixer setting the mixer can handle a feeder interruption for about 11 seconds without going under a concentration of 98% of the original API concentration in the ouflow of the mixer.

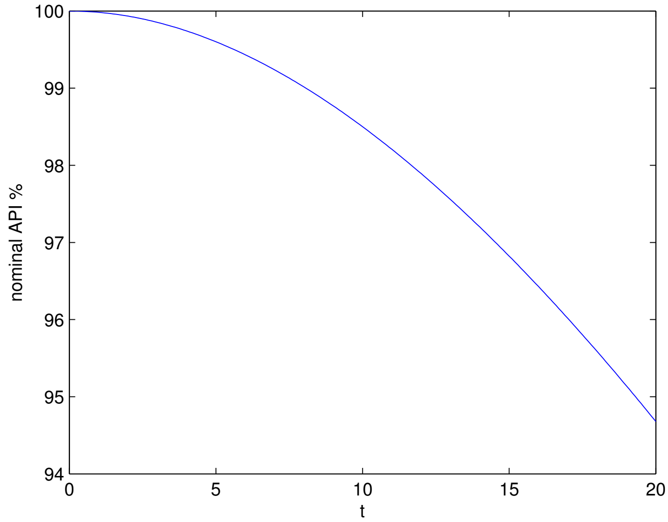

Figure 15: The predicted nominal concentration API in the ouflow of the mixer after a feeder stop, using the 2 CSTR in series model with $\tau = 54.33$. The x-axis represents time in seconds.

4.4 Damping ability

An important ability of a continuous mixer is its ability to smooth out and damp feed rate fluctuations. For the 2 CSTR in series model an analytical expression for the mixers ability to damp feed rate fluctuations was calculated (see APPENDIX A). A sinusoidal function was used to model the mass fraction of API in the inflow to the mixer.

$$c_{in} = A + Bsin(\omega t). \tag{30}$$

A sinusoidal function was selected as a model because it roughly approximates the nature of the mass concentration of API in the inflow produced by a feeder used in the experiments, see figure 16 for feeder data from a run A. The API output concentration for different values of ω is presented in figure 17. One can clearly see that higher frequency of the sinusoidal function results in higher damping, and a lower frequency of the in signal results in less damping.

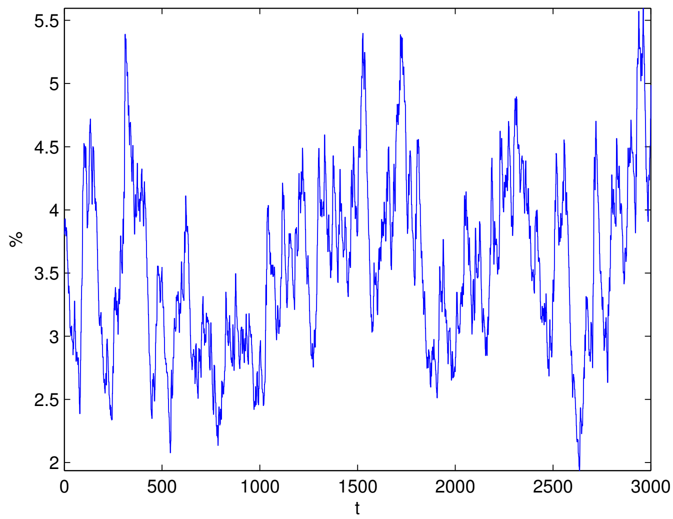

Figure 16: Mass fraction of how much of the powder going in to the mixer that was API during run A. The x-axis represents time in seconds.

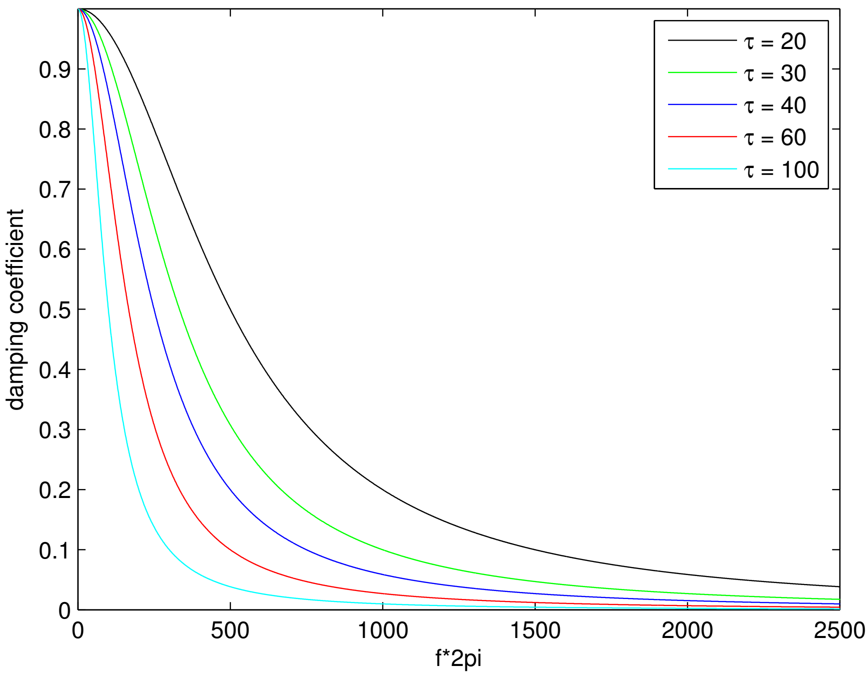

Figure 17: Relation between different frequencies of the fluctuations in the inflow and how it affects the damping ability of the mixer. The result is calculated for the 2 CSTR in series model for different values of τ. A damping coefficient of 0 means no damping and a damping coefficient of 1 means full damping. Full damping means that that there will be no fluctuation of the API concentration in the outflow. The parameter on the x-axis, $f * 2pi = \omega$.

4.4.1 Axial dispersion model with closed boundary conditions

A comparison between the axial dispersion model with closed and open boundary conditions was made. Real API concentration in the inflow from run D was used and the parameters in both models were set to $v = 0.0054$, $L = 1$, $D = 0.0007268$. In figure 18 the result of the simulation is presented. The result for both models are very similar with slightly more damping and longer residence time for the open boundary condition model. The similarity indicates that it does not matter if open or closed boundary conditions is used in this case. The result also shows that the mixer is able to smooth out large variations and keep the output concentration of API of around $4 \pm 1\%$.

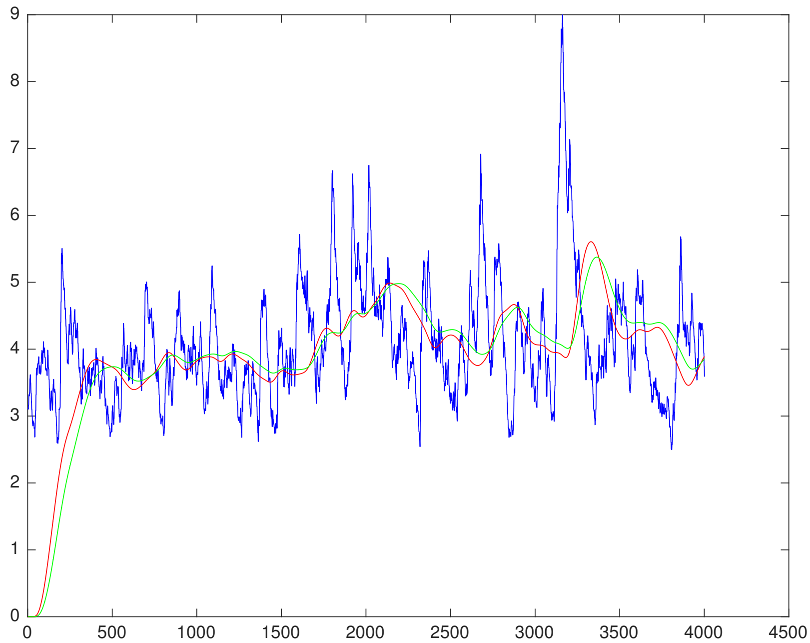

Figure 18: Simulation of run D using the axial dispersion model with closed boundary conditions solved by the finite difference method, the red line, and the convolution theorem together with the axial dispersion model with open boundary conditions, the green line. The y-axis represents

5 Conclusion

The optimal mixer settings depend on how much variability in the API concentration of the outflow that can be tolerated. A higher impeller rate results in a sharper RTD curve, which results in less mixing. For the blade angle that was used in the experiments, a higher number of blades results in a more spread out RTD curve and more mixing. If much variation can be tolerated, a faster impeller rate together with fewer blades can be used. As seen in figure 17 the frequency of the feed rate fluctuations is also important for how well the mixer will be able to smooth out fluctuations. A higher frequency results in a greater damping ability of the mixer and a lower frequency results in a smaller damping ability of the mixer.

The average absorbance method was used to extract information from the NIR data to get a measure of the amount of API in the powder mixture. The method was successful for pulse tests containing a higher mass, but for pulses with lower mass the method struggled to extract a clear pulse response.

The 2 CSTR in series model and the axial dispersion model with open boundary conditions were used to model the experimentally obtained RTD curves. The axial dispersion model fitted the data very well and was better than the 2 CSTR in series model for every run. The 2 CSTR in series model was also performing suitable well and can as well be used to model the flow.

The effect of interruptions in the API feedrate was also investigated. The results show that shorter interruptions can be tolerated without the need to discard tablets. If the interruptions however are too long, the mixer cannot maintain the API concentration in the outflow.

The models used in this thesis can be used to predict the API concentration in the outflow can if the concentration at the inlet is known. However the model only works if the residence time distribution of the mixer is known. Since the residence time distribution is related to the mixer settings, a new pulse test for each new setting has to be made. Since the residence time distributions are measured for when the powder flow is in a steady state, the models can not be used to say anything about the powder flow during start up or shut down. For this purpose more advanced methods are required.

References

[Ber04] H. Berthiaux. “Modeling Continuous Powder Mixing by Means of the Theory of Markov Chains”. In: *Particulate Science and Technology* 22 (4 2004), pp. 379–389.

[Gao11] Yijie Gao. “Characterizing continuous powder mixing using residence time distribution”. In: *Chemical Engineering Science* 66 (3 2011), pp. 417–425.

[Jaj13] Dalibor Jajcevic. “Large-scale CFD–DEM simulations of fluidized granular systems”. In: *Chemical Engineering Science* 98 (1 2013), pp. 298–310.

[Flo15] Algarin Florian. “Blend uniformity and powder phenomena inside the continuous tumble mixer using DEM simulations”. In: *Particulate Science and Technology* 61 (3 2015), pp. 792–801.

[Eng16] William Engisch. “Using Residence Time Distributions (RTDs) to Address the Traceability of Raw Materials in Continuous Pharmaceutical Manufacturing”. In: *Journal of Pharmaceutical Innovation* 11 (1 2016), pp. 64–81.

APPENDIX A

An analytical expression for the concentration of API in the outflow is calculated for the 2 CSTR in series and from this formula a damping coefficient is deduced.

The concentration of API in the inflow is approximated by

$$c_{in}(t) = A + Bsin(\omega t) \tag{31}$$

The motivation of why choosing a sinus function can be found in section 4.3.2. From equation 5, the RTD function for 2 CSTR in series is given by

$$E(t) = b^2 te^{-bt}. \tag{32}$$

With $b = 1/\tau$. Using the convolution theorem, equation 4, together with equation 26 and equation 27 gives

$$c_{out}(t) = \int_0^t (A + Bsin(\omega x))b(t-x)\exp(-b(t-x))dx \tag{33}$$

The integral was solved by Mathematica and the out concentration can be expressed as

$$c_{out}(t) = A - Ae^{-bt}(1+bt) + \frac{b^3 B}{(\omega^2+b^2)^2}\Big(e^{-tb}(\omega(\omega^2+b^2)t+2) + sin(\omega t)(b^2-\omega^2) - cos(\omega t)2\omega b\Big) \tag{34}$$

To find how much the in signal is damped the max of the in signal is compared with the max of the out signal when steady state is reached. Steady state for c_{out} is obtained by letting $t \to \infty$.

$$c^s_{out}(t) = A + \frac{b^3 B}{(\omega^2+b^2)^2}\Big(sin(\omega t)(b^2-\omega^2) - cos(\omega t)2\omega b\Big) \tag{35}$$

where s denotes steady state. To find extreme points of c_{out}, the function is differentiated and set equal to 0.

$$\frac{d}{dt}c^s_{out}(t) = \frac{b^3 B}{(\omega^2+b^2)^2}\Big(cos(\omega t)\omega(b^2-\omega^2) + sin(\omega t)2\omega^2 b\Big) = 0 \tag{36}$$

This can be written as

$$tan(\omega t + n\pi) = \frac{\omega^2 - b^2}{2\omega b}, n = 1,2,... \tag{37}$$

with solutions

$$t_{extreme} = arctan\Big(\frac{\omega^2-b^2}{2\omega b}\Big) + \frac{n\pi}{\omega}. \tag{38}$$

With $n = 0$ we can now write the the maximum out concentration as

$$c^s_{out}(t) = A + \mid \frac{b^2 B}{(\omega^2 + b^2)^2}\Big(sin(\omega t_{extreme})(b^2 - \omega^2) - cos(\omega t_{extreme})2\omega b\Big) \mid \quad (39)$$

MATLAB CODE

```
% Loading of all measurements from the near infrared
% absorption spectrum from run A. Same was done for all  runs.

[fileName,dirName]=uigetfile('runA.xlsx');
[~,~,rawData] = xlsread(fullfile(dirName,fileName));
dataA2 = cellfun(@str2double,rawData);

% Removing not a number values from run A. Same was done for all runs.

dataA2stripped = dataA2(1821:end,:);
tA = [1:size(dataA2,1)];
tAstripped = tA(1821:end);

for j = 1:size(dataA2stripped,2)
    nans = isnan(dataA2stripped(:,j));
    for i = 1:size(dataA2stripped,1)
        if(nans(i))
            dataA2stripped(i,j) = dataA2stripped(i-1,j);
        end
    end
end

% Extracting the pulse response for run A. Same was done for all runs.

meanVectorA = mean(transpose(dataA2stripped));
standardDeviationA = std(transpose(dataA2stripped));

dataA2strippedSnv = dataA2stripped;

for i = 1:size(dataA2stripped,1)
    dataA2strippedSnv(i,:) = (dataA2stripped(i,:)
    - meanVectorA(i))/standardDeviationA(i);
end

topDataA = dataA2strippedSnv(:,157:162);
topDataMeanA = mean(transpose(topDataA));

% Extraction of the RTD curve for run A.
```

```
RTDA =
(topDataMeanA(1574:2027)-0.3772)/trapz((topDataMeanA(1574:2027)-0.3772));

% Parameter estimation of the 2 CSTR in series model.
% Same was done for all runs.

tA1 = [1:454];
t = [0:500];

pecletNumbers = [1:8];

funA = @(PA) RTD(tA1,PA(1),PA(2),PA(3)) - RTDA;
[PA_estimated1, resnormA] = lsqnonlin(funA,[0.05,0.2,1]);
yA_estimated1 = RTD(t,PA_estimated1(1),PA_estimated1(2),PA_estimated1(3));
pecletNumbers(1) = PA_estimated(1)*PA_estimated(3)/PA_estimated(2);

% Parameter estimation of the axial dispersion model.
% Same was done for all runs.

t = [1:(stop-start)+1];
u = 0.2;
D = 0.5;
L = 1;

fun = @(P) RTD(t,P(1),P(2),P(3)) - normalizedData;
P_estimated = lsqnonlin(fun,[0.05,0.2,0.5]);
y_estimated = RTD(t,P_estimated(1),P_estimated(2),P_estimated(3));

% Axial dispersion model solved by the finite
% difference method

dataN7 = xlsread('N7.xlsx');
inSignal = dataN7(1000:5000,7);
% Define the grid
n = 4000; % number of time spaces
m = 1600; % number of room spaces


% Define parameters
v = 0.5;
D = 0.1;
```

```
L = 100; % Length of mixer 1
T = 4000;
dt = T/n;
dx = L/m;
t = [0:dt:T];
x = [0:dx:L];
k1 = v*dt/(dx);
k2 = D*dt/(dx*dx);

% Time-step matrix
B = zeros(m+1);

for i = 2:m
    B(i,i-1) = -k1-k2;
    B(i,i) = 1+k1+2*k2;
    B(i,i+1) = -k2;
end
B(1,1) = 1;
B(m+1,m+1) = 1;


%Initial conditions
b1 = ones(1,2000);
b2 = zeros(1,200);
b3 = ones(1,2601);
B1 = [b1 b2 b3];


% Algorithm
for i = 2:n+1
    c1(i-1,1) = B1(i);
    c1(i,:) = B\c1(i-1,:)';
    c1(i,m+1) = c1(i,m);
end


% Analytical feeder interruption
time = 0:0.1:20;

syms f(t) x;
```

```
f(t) = 100*(1-int(x/24.33^2*exp(-x/24.33),0,t));



values = time;
for i = 1:length(time)
    values(i) = double(f(time(i)));
end

figure(1)
plot(time(1:201),values)
ylabel('nominal API %')
xlabel('t')
axis([0 20 94 100])
```